

Exploring shallow sunspot formation by using Implicit Large-eddy simulations

F. J. Camacho^{1,*}, G. Guerrero^{1,**}, P. K. Smolarkiewicz²,
A. G. Kosovichev³ and N. N. Mansour⁴

¹Universidade Federal de Minas Gerais, Av. Pres. Antônio Carlos, 6627 - Pampulha
Belo Horizonte - MG, Brazil

*email: camacho@fisica.ufmg.br

**email: guerrero@fisica.ufmg.br

²European Centre for Medium-Range Weather Forecasts, Reading RG2 9AX, UK
email: smolar@ecmwf.int

³New Jersey Institute of Technology, Newark, NJ 07103, USA
email: alexander.g.kosovichev@njit.edu,

⁴NASA, Ames Research Center, Moffet Field, Mountain View, CA, USA
email: nagi.n.mansour@nasa.gov

Abstract. The mechanism by which sunspots are generated at the surface of the sun remains unclear. In the current literature two types of explanations can be found. The first one is related to the buoyant emergence of toroidal magnetic fields generated at the tachocline. The second one states that active regions are formed, from initially diffused magnetic flux, by MHD instabilities that develop in the near-surface layers of the Sun. Using the anelastic MHD code EULAG we address the problem of sunspot formation by performing implicit large-eddy simulations of stratified magneto-convection in a domain that resembles the near-surface layers of the Sun. The development of magnetic structures is explored as well as their effect on the convection dynamics. By applying a homogeneous magnetic field over an initially stationary hydrodynamic convective state, we investigate the formation of self-organized magnetic structures in the range of the initial magnetic field strength, $0.01 < B_0/B_{eq} < 0.5$, where B_{eq} is the characteristic equipartition field strength.

Keywords. convection, EULAG-MHD, ILES, turbulence, sunspots

1. Anelastic Turbulent Convection with EULAG-MHD

We use the code EULAG-MHD which solves an MHD extension of the Lipps & Hemler (1982) anelastic equations (see Smolarkiewicz & Charbonneau 2013).

$$\frac{d\vec{u}}{dt} = -\nabla\pi' - \vec{g}\frac{\theta'}{\theta_0} + \frac{1}{\mu\rho_0}\vec{B} \cdot \nabla\vec{B}, \quad (1.1)$$

$$\frac{d\theta'}{dt} = -\vec{u} \cdot \nabla\theta_e - \alpha\theta', \quad (1.2)$$

$$\frac{d\vec{B}}{dt} = \vec{B} \cdot \nabla\vec{u} - \vec{B}\nabla \cdot \vec{u}, \quad (1.3)$$

$$\nabla \cdot (\rho_0\vec{u}) = 0, \quad (1.4)$$

$$\nabla \cdot \vec{B} = 0. \quad (1.5)$$

Here, θ is the potential temperature, tantamount of the specific entropy ($s = c_p \ln \theta$). Subscripts “o” denote an isentropic base state in hydrostatic balance. Primes denote perturbations around an ambient state (denoted by subscript “e”), and \vec{g} is a constant gravitational acceleration. π' is a density normalized pressure perturbation encompassing

the hydrostatic and magnetic pressure. The domain of the simulations is a rectangular box with dimensions $50 \times 50 \times 20 \text{ Mm}^3$ in the xyz axes, respectively. In the x and y directions we use periodic boundary conditions. For the z direction, the bottom of the domain is taken where $z = 0 \text{ Mm}$ and the top where $z = 20 \text{ Mm}$. We use two 3D grids at low and high resolution, 128^3 and 256^3 meshpoints, respectively. For the ambient state we choose a three-layer polytropic atmosphere given by the equations:

$$\frac{dT_e}{dz} = \frac{-g_0}{R_g(m(z) + 1)} \quad (1.6)$$

$$\frac{d\rho_e}{dz} = \frac{\rho_e}{T_e} \left(\frac{-g_0}{R_g} - \frac{dT_e}{dz} \right), \quad (1.7)$$

where the layers are connected via smooth transitions in the polytropic index profile, $m(z)$. The vertical stratification given by eqs. (1.6) and (1.7) leads to a convectively stable layer at the bottom $0.0 < z < 0.2 \text{ Mm}$, followed by an adiabatic layer $0.2 < z < 1.8 \text{ Mm}$, and a convection-unstable layer at the top, $1.8 < z < 2.0 \text{ Mm}$. The last term on the rhs of (1.2) is a Newtonian cooling that models the divergence of the non-computable Reynolds heat flux. It relaxes θ' toward zero within a time-scale, $\tau = \alpha^{-1}$

$$\frac{d}{dz} \rho_0 \langle w' \theta' \rangle = -\rho_0 \alpha \theta'. \quad (1.8)$$

For the simulations performed in this work we consider $\tau = 1.1$ days. We impose a uniform vertical magnetic field, $\vec{B} = (0, 0, B_0)$, of three different strengths over a HD convective pattern in steady state. The three different strengths for the imposed magnetic field are $B_0/B_{eq} = (0.01, 0.1, 0.5)$, for the low resolution HD simulation, and $B_0/B_{eq} = (0.05, 0.1, 0.5)$, for the high resolution simulation. Here, B_{eq} is the equipartition magnetic field:

$$\frac{1}{2\mu_0} B_{eq}^2 = \frac{1}{2} \bar{\rho} u_{rms}^2. \quad (1.9)$$

2. Results

From the cases considered, only the low resolution simulation with $B_0/B_{eq} = 0.1$, and the high resolution simulations with $B_0/B_{eq} = 0.05$ and $B_0/B_{eq} = 0.1$, show the formation of localized magnetic flux concentrations. The most representative results are obtained for the low resolution simulation with $B_0/B_{eq} = 0.1$, shown in Figures 1 and 2. The simulations with imposed vertical magnetic field reveal that there is an optimal range of field strengths, $0.01 < B_0/B_{eq} < 0.5$, for the formation of localized magnetic flux concentrations. Vertically, these structures have the length scale of the entire adiabatic layer. For the cases with a stronger imposed magnetic field, the flow pattern loses the convective structure.

For the simulations that show the formation of magnetic flux concentrations, an important change in the form of the convective cells is observed. At the upper layers ($z > 18.8 \text{ Mm}$), the convective cells near the magnetic flux concentrations acquire an elongated shape pointing towards the center of these structures. This is reminiscent of the penumbra around the dark center of sunspots (e.g., Borrero & Ichimoto 2011).

For the moment, it is not clear whether these structures are the results of MHD instabilities or the collapse of the magnetic flux in the downflow lanes. Since the downflows have the horizontal scale of the deep convective motions, the magnetic elements at the surface cover several small-scale convective elements.

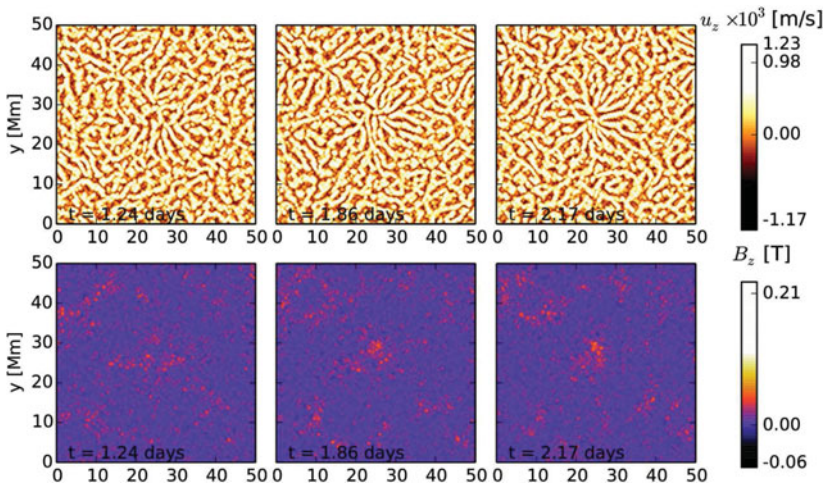


Figure 1. xy snapshots, at 1.2 Mm below the top boundary, of the vertical velocity and magnetic field at different times for the low resolution simulation with $B_0/B_{eq} = 0.1$.

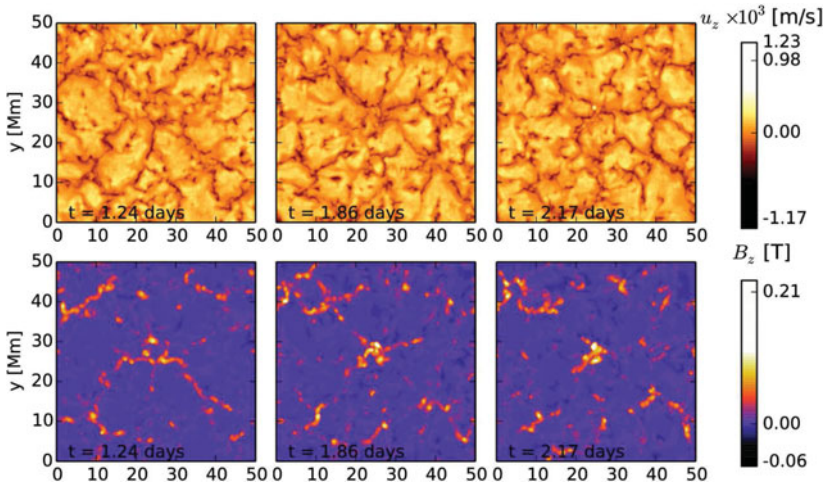


Figure 2. xy snapshots, at 4.4 Mm below the top boundary, of the vertical velocity and magnetic field at different times for the low resolution simulation with $B_0/B_{eq} = 0.1$.

Acknowledgements

Special thanks to the organizer for a wonderful meeting and to the IAU for travel support. This work was partly funded by FAPEMIG grant APQ-01168/14 (FC and GG). The simulations were performed in the NASA cluster Pleiades and Brazilian supercomputer Sdumont of the National Laboratory of Scientific Computation (LNCC).

References

- Smolarkiewicz, P. K., & Charbonneau, P. 2013, *J. Comput. Phys.*, 236, 608
 Lipps F.B., Hemler R.S., A scale analysis of deep moist convection and some related numerical calculations, *J. Atmos. Sci.*, 39 (1982) 2192-2210
 Borrero J. M. & Ichimoto K., Magnetic Structure of Sunspots, *Living Rev. Solar Phys.*, 8, (2011), 4.